Research Article

Aysegul Kaymak Ozdemir* and Mahinur Basci

Elucidating the role of ZRF1 in monocyte-to-macrophage differentiation, cell proliferation and cell cycle in THP-1 cells

https://doi.org/10.1515/tjb-2024-0015
Received January 17, 2024; accepted February 1, 2024;
published online March 21, 2024

Abstract

Objectives: ZRF1 (Zuotin-related factor 1) is a versatile protein engaged in protein folding, gene regulation, cellular differentiation, DNA damage response, and immune system and cancer development regulation. This study investigates the role of ZRF1 in monocyte-to-macrophage transformation, and its effects on cell proliferation and the cell cycle.

Methods: We generated ZRF1-depleted THP-1 cells and induced macrophage differentiation using phorbol 12-myristate 13-acetate (PMA). Differentiation was assessed via microscopy and flow cytometry, while cell proliferation was quantified with the [3-(4,5-dimethylthiazol-2-yl)-5-(3-carboxymethoxyphenyl)-2-(4-sulfophenyl)-2H-tetrazolium, inner salt] (MTS) assay, and the cell cycle was analyzed through flow cytometry using propidium iodide staining.

Results: ZRF1-depleted THP-1 cells exhibited notable morphological changes. Flow cytometry post-PMA treatment indicated these cells were smaller and less granular than controls. Proliferation rates of ZRF1-depleted monocytes and macrophages were significantly higher than controls, particularly over longer durations. Cell cycle analysis showed ZRF1 depletion notably affected the G0-G1 phase, highlighting its significant role in macrophage differentiation.

Conclusions: The findings provide important insights into ZRF1's role in monocyte-to-macrophage differentiation and its impact on cell proliferation and the cell cycle. This research not only supports existing knowledge about ZRF1 but also enhances our understanding of its multifaceted roles in cellular processes.

Keywords: ZRF1; THP-1 cells; PMA; monocyte to macrophage differentiation; cell cycle

Introduction

Zuotin-related factor 1 (ZRF-1), also known as DnaJ heat shock protein family (Hsp40) member C2 (DNAJC2), M-phase phosphoprotein 11 (MPP11), or heat shock protein 40 (HSP40), has emerged as a multifunctional protein which is involved in a plethora of biological processes including protein folding, gene regulation [1, 2], cellular differentiation and development, deoxyribonucleic acid (DNA) damage response [3, 4], regulation of immune system and cancer development. Specifically, ZRF1 interacts with monoubiquitinated histone H2A, displacing the polycomb-repressive complex 1 (PRC1) from chromatin, which results in the transcriptional activation of typically silenced genes, particularly in stem and cancerous cells [2, 5]. As a member of the Dnaj/HSP family, ZRF1 is part of the mammalian ribosome-associated complex (mRAC) [6] and acts as a molecular chaperone for nascent polypeptide chains emerging from the ribosome [7].

The presence of Dnaj domains across diverse organisms underscores this family's evolutionary significance in differentiation and development [8]. In neural progenitor cells, ZRF1 upregulates neural markers such as Pax6 and maintains Wnt ligand expression crucial for cell self-renewal [9]. It also interacts with the inhibitor of differentiation protein 1 (Id1) to regulate neural gene activation during stem cell differentiation [10]. Additionally, ZRF1 is important for seed development in Arabidopsis [11] and is crucial for the formation of mesoderm-derived tissues, like the heart, in mammals [12]. The indispensability of ZRF1 in early development is further demonstrated by the early post-implantation lethality observed in mouse embryos where the ZRF1 gene is invalidated using the Crispr/Cas9 approach [13].

ZRF1 plays a crucial role in senescence, particularly due to its involvement in the cell cycle. Research focusing on the

***Corresponding author: Aysegul Kaymak Ozdemir**, Department of Biochemistry, Faculty of Pharmacy, Ege University, Bornova, Izmir, 35040, Türkiye, Phone: +90 5468135867, E-mail: aysegul.kaymak.ozdemir@ege.edu.tr. https://orcid.org/0000-0001-5153-9602

Mahinur Basci, Department of Biotechnology, Faculty of Science, Ege University, Izmir, Türkiye, E-mail: mahinur.basci@gmail.com. https://orcid.org/0009-0002-3826-2113

effects of S6 kinase within the context of the mammalian target of rapamycin complex 1 (mTORC1) pathway has identified ZRF1 as a target of S6 kinase. The study revealed that reducing ZRF1 expression led to decreased senescence, while its overexpression restored the senescence process through the upregulation of $p16^{INK4A}$ [14]. This gene is pivotal in inhibiting cyclin D-dependent protein kinases, thereby regulating the G1-S phase transition [15]. Complementing this, another investigation demonstrated ZRF1 as a transcriptional activator of the *INK4-ARF* locus, responsible for encoding genes such as $p14^{ARF}$, $p15^{INK4B}$, and $p16^{INK4A}$, by recruiting specific deubiquitinases to the chromatin. Consequently, ZRF1 depletion in cells with oncogenic H-Ras hampers the expression of $p16^{INK4A}$ and $p14^{ARF}$, facilitating the circumvention of senescence [16]. Furthermore, ZRF1's role extends to binding G-quadruplex DNA structures post-ultraviolet (UV) irradiation, which is vital for preventing UV-induced senescence, and positioning ZRF1 as a key regulator in cellular responses to DNA damage and stress [17].

ZRF1's involvement in cancer is multifaceted, influencing disease progression, metastasis, therapeutic response, and potential as a diagnostic marker. In breast cancer, it acts as a potential early diagnostic marker, with increased autoantibody responses seen in patients, particularly in invasive ductal carcinoma and less aggressive tumors [18]. Additionally, ZRF1 depletion in breast cancer leads to increased metastatic behavior and reduced responsiveness to antihormonal therapy and chemotherapy [19]. In colorectal [20] and gastric cancers [21], ZRF1 overexpression correlates with enhanced tumor growth, cell proliferation, and invasion. In acute myeloid leukemia (AML), ZRF1 depletion results in decreased cell proliferation, increased apoptosis, and enhanced differentiation [22], suggesting its therapeutic targeting potential. In line with that, ZRF1 is identified among the sixteen leukemia-associated antigens in both chronic myeloid leukemia (CML) and AML patients [23], and demonstrated as a prime target for T cell-based immunotherapy [24]. Furthermore, Yi et al. reveals that the HSP70L1 protein, which enhances immune responses as an extracellular adjuvant but suppresses dendritic cell maturation intracellularly through repressive histone modifications, relies on its interaction with ZRF1 for stability and function [25].

The fact that ZRF1 is involved in the development of mesoderm-derived tissues, its abnormal expression is associated with blood and bone marrow cancers, and that it epigenetically regulates dendritic cell (DC) differentiation suggests that ZRF1 has an unexplored function in the context of immune cell differentiation, especially those of myeloid origin. Hence, we aim to characterize the effect of ZRF1 on the differentiation of monocytes into macrophages, one of the most important innate immune cells in host defense, and to investigate its specific effects on cell proliferation and cell cycle.

Materials and methods

Cell lines and culture conditions

THP-1 cells and human embryonic kidney 293 cells (HEK293T) were kind gifts from Prof. Dr. Güneş Esendağlı and Prof. Dr. Şerif Şentürk, respectively. THP-1 cells were maintained in Roswell Park Memorial Institute (RPMI, Gibco) supplemented with 10 % fetal bovine serum (FBS, Gibco) and penicillin/streptomycin (Gibco) at 37 °C with 5 % carbone dioxide (CO_2). HEK293T cells were maintained in Dulbecco's Modified Eagle's Medium (DMEM, Gibco) supplemented with 10 % FBS (Gibco), L-glutamine (Gibco) and penicillin/streptomycin (Gibco).

Transfections and lentiviral infection

The scrambled plasmid was a kind gift from Prof. Dr. Şerif Şentürk, while the pCM.dR8.91 (packaging), vesicular stomatitis virus G protein (VSV-G, envelope), and short hairpin for ZRF1 (shZRF1) plasmids (TRCN0000254055 and TRCN0000254058) were generously provided by Dr. Luciano Di Croce. To generate lentiviruses carrying short hairpin ribonucleoid acid (shRNA), HEK293T cells were cultured until reaching 80 % confluency. Approximately 5–6 × 10^6 HEK293T cells were transfected using the polyethylenimine (PEI) method with 6 µg of pCM.dR8.91, 5 µg of VSV-G, and 7 µg of shScrambled, shRNA#55 (TRCN0000254055), or shRNA#58 (TRCN0000254058) plasmids. At 54 h posttransfection, the medium containing viral particles was harvested, filtered through 0.45 µm filters, and stored at −80 °C until the infection process. The viral medium was then applied to six-well plates, each containing 5 × 10^5 THP-1 cells, and subjected to centrifugation at 1000 g for 2 h at 24 °C (spinofection). Subsequently, the medium was replaced, and cells were cultured in fresh virus-free medium for 48 h. After this incubation period, the infection step was repeated, and cells were allowed to recover for 72 h. Knockdown cells were selected using 1 µg/mL puromycin and maintained under constant puromycin selection.

Macrophage differentiation protocol

THP-1 monocytes were seeded in six-well plates at a density of 5 × 10^5 cells/2 mL per well. To induce macrophage differentiation, cells were treated with phorbol 12-myristate 13-acetate (PMA, Enzo) at concentrations of 5, 10, 50 or 100 ng/mL. Incubations of 24, 48 or 72 h with the indicated doses of PMA were tested, followed by a rest period of 24 or 48 h in RPMI medium. Differentiated cells were evaluated for morphological changes, adhesion to the cell culture dish and flow cytometry analysis. Morphological changes were examined under the Olympus CKX41 microscopy.

Quantitative reverse transcription polymerase chain reaction (qRT–PCR) analysis

RNA extraction was performed using Trizol (Invitrogen) following the provided instructions. The purity and quantity of the extracted RNAs were assessed using a spectrophotometer (Perkin Elmer and Thermo) based on absorption values at 260 and 280 nm wavelengths. Complementary DNA (cDNA) was synthesized from 2 µg of RNA using the First Strand cDNA synthesis kit (Applied Biosystems). The cDNA was then diluted to 200 µL with nuclease-free water, and 2 µL samples were utilized for each qRT-PCR reaction employing asymmetrical cyanine dye green (SYBR, Promega, GoTaq PCR Master Mix). The qRT-PCR primers employed were as follows: S18 forward: 5′-GAACTCACTGAGGATGAGGTGG-3′, S18 reverse: 5′-CTGGGATCTTGTACTGGCGT-3′; ZRF1 forward: 5′-CGAAGTGT-TTACCCCAGTGTT-3′, ZRF1 reverse: 5′- TCTCCTCTCATCACGACATTCTG-3′. After the qPCR reaction, mRNA expression levels were determined using the delta cycle threshold (CT) method, and the fold change was calculated as the $2^{-\Delta\Delta CT}$ value from the formula ΔΔCT=ΔCT treatment − ΔCT control.

Western blot analysis

Cell pellets were harvested and resuspended in radioimmunoprecipitation (RIPA) buffer (Intron) containing protease (Bioshop) and phosphatase (Thermo Halt) inhibitors, adjusted to the pellet size. Following a 45 min incubation on ice with periodic vortexing every 5 min, the samples underwent centrifugation at 14,000 rpm at 4 °C. Supernatants were carefully collected, and protein concentrations in each sample were determined using the bicinchoninic acid (BCA) protein assay kit (Takara). Subsequently, 20 µg of protein was loaded onto a 10 % sodium dodecyl-sulfate polyacrylamide gel electrophoresis (SDS-PAGE) gel for western blot analysis. Antibodies against B-actin (CST) and Dnajc2 (Thermo) were employed to detect the respective proteins. Relative band intensities were quantified using the ImageJ program.

Cell proliferation assay

THP-1 cells were seeded in 96-well plates at densities of 2.5×10^3 cells/100 µL per well for monocytes and 10×10^3 cells/100 µL per well for macrophage experiments, with five replicates each. Cell numbers corresponding to specific days were determined using the [3-(4,5-dimethylthiazol-2-yl)-5-(3-carboxymethoxyphenyl)-2-(4-sulfophenyl)-2H-tetrazolium, inner salt] (MTS) assay (CellTiter 96 AQueous One Solution Cell Proliferation). Following the addition of MTS solution at 1/5 volume of the cell culture medium and a 3.5 h incubation at 37 °C in the dark, the absorbance of each well was measured at 570 nm using a Varioskan plate reader. Cell numbers were calculated as fold change compared to control samples after subtracting background absorbance.

Cell cycle analysis

For cell cycle analysis, THP-1 monocytes were harvested, washed with 1x phosphate-buffered saline (PBS), and fixed with 70 % ethanol. In contrast, THP-1 macrophages were collected by a brief trypsin treatment followed by an incubation at 37 °C for 30–45 min. Subsequently, they were washed with 1x PBS and fixed with 70 % ethanol. Both cell types were stored at −20 °C until analysis by flow cytometry. For propidium iodide (PI) staining, 1×10^6 cells were counted and resuspended in 100 µL of PI staining solution, comprising 0.5 µL RNAse A (Thermo: 5 µg RNAse per sample), 5 µL PI solution (eBioscience: 40 µg of PI per sample), and 0.1 % Triton-X in 1x PBS. After an incubation of 30–60 min at room temperature in the dark, samples were analyzed using the BD (Becton, Dickinson) LSR Fortessa at the Flow Cytometry and Cell Sorting Unit at İzmir Biomedicine and Genome Center. The cell cycle of the cells was analyzed using the FlowJo program.

Flow cytometry

To determine the percentage of differentiated cells, monocytes and macrophages were collected as previously described. Cells were then suspended in 1 mL of blocking buffer, composed of 5 % FBS in 1x PBS, and incubated on ice for 30 min. Following centrifugation at 1000 g at 4 °C, cells were adjusted to a concentration of 1 x 10^6 cells/100 µL blocking buffer, supplemented with 1 µL of cluster of differentiation molecule 11b-Allophycocyanin (CD11b-APC, eBiosciences) antibody per sample, and incubated on ice for 60 min in the dark. After washing three times with blocking buffer, cells were resuspended in 500 µL 1x PBS and analyzed using the BD (Becton, Dickinson) FACSCanto II at the Flow Cytometry and Cell Sorting Unit at İzmir Biomedicine and Genome Center.

Statistical analysis

Data were presented in forms of mean±standard error of means of three biological replicates. GraphPad Prism 8.0 software (GraphPad Software Inc.) was used to analyze the data. Unpaired student's *t*-test was used for comparisons. *p<0.05, **p<0.01, ***p<0.001, and ****p<0.0001 were considered to indicate a statistically significant difference.

Results

Establishment of ZRF1 depleted THP-1 cells

To investigate the function of ZRF1 in monocytes and macrophages, THP-1 cells were chosen due to their widely usage in monocyte-macrophage related studies and acceptance in the literature [26–29]. THP-1 cells expressing either a control (shScrambled) or two distinct shRNAs targeting ZRF1 (shZRF1#55 and shZRF1#58) were generated by viral infection. The reduction in ZRF1 mRNA was assessed using qRT-PCR, revealing an 80 % gene knockdown with both plasmids (Figure 1A). Western blot analysis was conducted on protein samples to validate these findings, showing a 50 % knockdown with the shZRF1#55 plasmid and a 90 % knockdown with the shZRF1#58 plasmids in comparison to the control cells (Figure 1B and C). Furthermore, microscopic examination of the morphological characteristics of the three cell lines indicated no significant alterations due to viral infection in the THP-1 cells, thereby confirming the reliability of the experimental setup (Figure 1D).

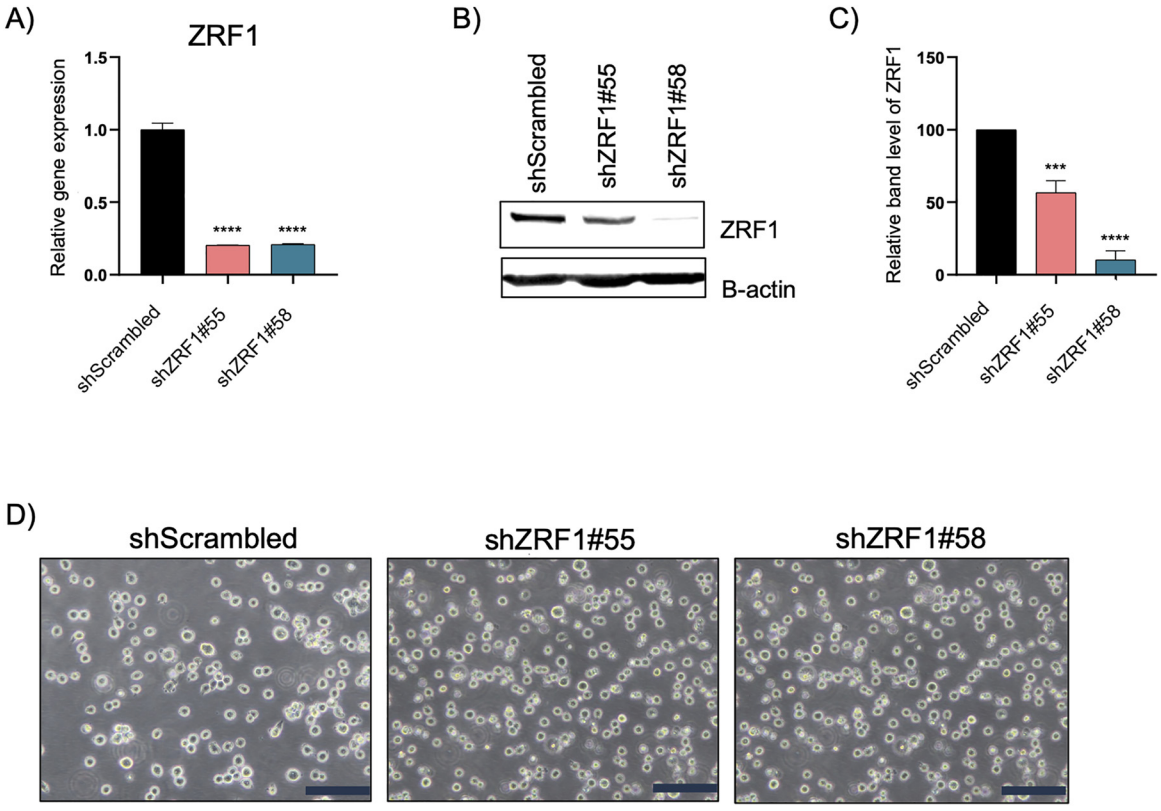

Figure 1: Establishment of ZRF1 depleted THP-1 cells. (A) qRT-PCR analysis of ZRF1 after viral induction with two distinct plasmids. S18 was used as a housekeeping gene. Data represent the average of three experiments, ± S.E.M. ****p<0.0001, calculated by two-tailed unpaired t test. (B) Western blot analysis for ZRF1 after viral induction. B-actin was used as a loading control. (C) Relative band intensity of ZRF was quantified by the ImageJ program. Data represent the average of three experiments, ± S.E.M. ***p<0.001, and ****p<0.0001, calculated by two-tailed unpaired t test. (D) Brightfield images of THP-1 cells after viral infection with different plasmids. Scale bars, 200 µm.

Evaluation of ZRF1's effect on monocyte-to-macrophage differentiation in THP-1 cells upon PMA treatment

After verifying ZRF1 knockdown using two different plasmids, the macrophage differentiation protocol was optimized by first testing the dose and incubation times of PMA on wild-type THP-1 cells at various doses and times after careful review of the literature [30–33]. The PMA concentrations tested ranged from 5 ng/mL to 100 ng/mL, with incubation periods extending from 24 to 72 h. The transition from monocytes to macrophages typically involves an increase in cell size, granularity, and expression of cell surface marker CD11b. To assess the effectiveness of PMA in inducing THP-1 monocytes to differentiate into macrophages, flow cytometry was employed [34], comparing the forward scatter area (FSC-A) and side scatter area (SSC-A) between THP-1 monocytes and macrophages (Figure 2A). As shown in Figure 2B, a notable escalation in both size and granularity was observed over time. The expression of CD11b markedly transitioned from left to right following 72 h of incubation with PMA. Nonetheless, due to concerns regarding toxicity, a concentration of 100 ng/mL PMA for 48 h was selected for subsequent differentiation experiments. To evaluate ZRF1's effect on monocyte-to-macrophage differentiation, both control and ZRF1 depleted THP-1 cells were subjected to PMA-induced differentiation, with their morphological changes monitored over a 48-h period (Figure 3). Within 24 h of PMA treatment, nearly all cells had adhered to the cell culture dishes. Cell clustering, a hallmark of macrophage differentiation, was evident in all three cell types. Notably, while the control cells appeared small and round, the ZRF1 depleted cells exhibited a rather larger and spiky morphology. PMA treatment of THP-1 cells is commonly viewed as a priming phase. Allowing the cells to rest post-PMA stimulation typically results in a morphology characteristic of classically activated macrophages [30]. To determine if there is a similar pattern in our case, PMA-differentiated cells were allowed to rest and observed for 48 h (Figure 4). Consistent with existing literature, the THP-1 cells exhibited a morphology like M1-polarized macrophages, characterized by a classic elongated spindle-shaped appearance.

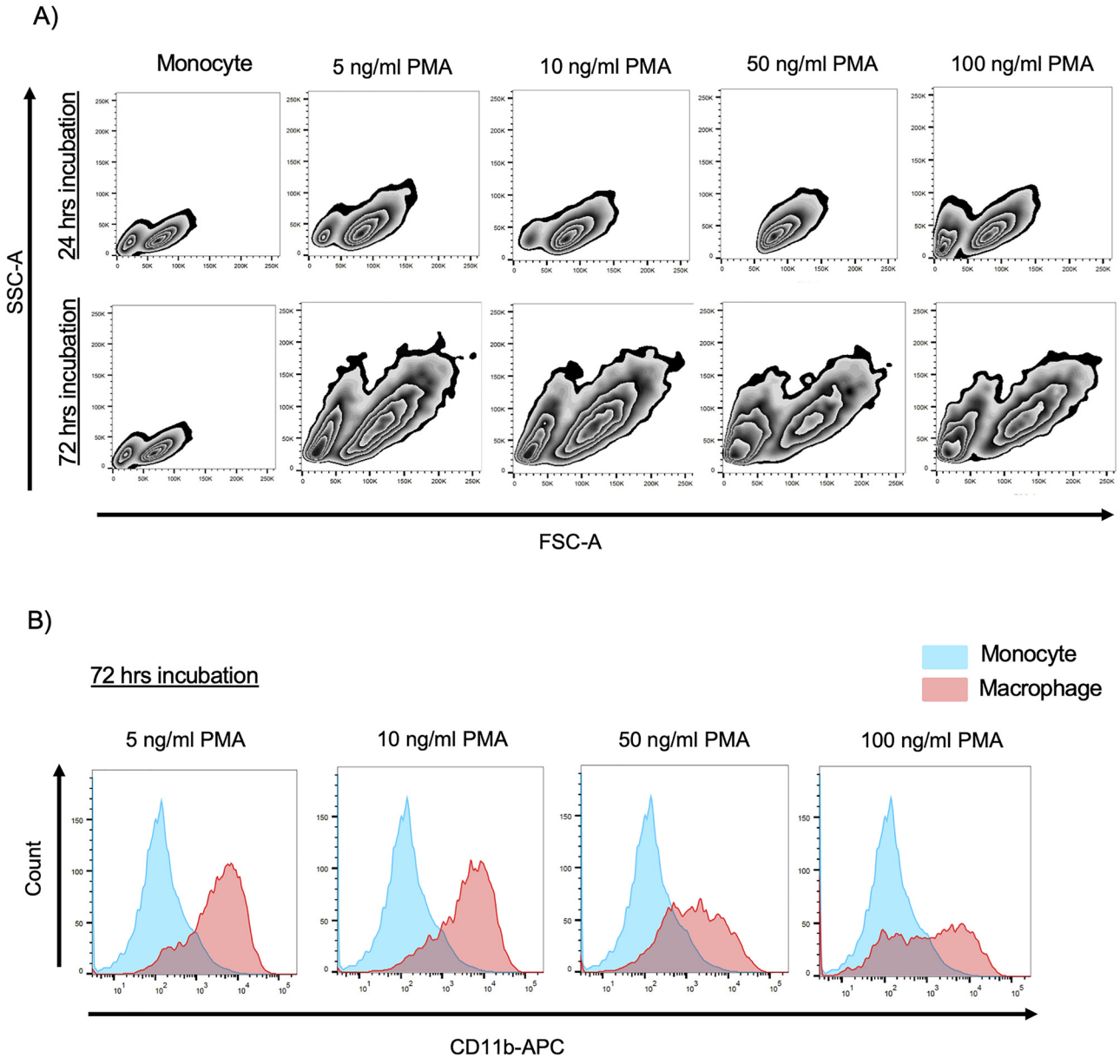

Figure 2: Optimization of macrophage differentiation protocol for THP-1 monocytes. (A) Comparison of flow cytometric cell features between THP-1 monocytes upon treatment with PMA by zebra plots displaying side scatter area (SSC-A) on the y-axis against forward scatter area (FSC-A) on the x-axis. In this plot, FSC-A is indicative of cell size, while SSC-A reflects the intensity of cytoplasmic granularity. (B) Histogram analysis of CD11b-APC corresponding to increasing concentration and incubation time of PMA.

To further explore the role of ZRF1 in macrophage differentiation, cells either expressing control or shZRF1 plasmids were analyzed through flow cytometry following 24 and 48 h of treatment with PMA, and a subsequent 48 h rest period post-PMA treatment (Figure 5A). In assessing the FSC-A and SSC-A of THP-1 monocytes from three distinct cell lines, it was observed that ZRF1 depleted cells were generally smaller and exhibited less structural complexity compared to their ZRF1 expressing counterpart. With the extension of the incubation period, all groups of cells demonstrated an increase in size and complexity, which became particularly marked after the 48 h rest period post-PMA exposure. Intriguingly, THP-1 cells expressing shZRF1#58, which exhibited higher levels of ZRF1 knockdown, showed a more diverse population in size and complexity relative to the ZRF1 expressing control cells, suggesting potential discrepancies in macrophage differentiation. On the other hand, THP-1 cells with lower levels of ZRF1 knockdown (expressing shZRF1#55) displayed characteristics between the ZRF1-expressing control cells

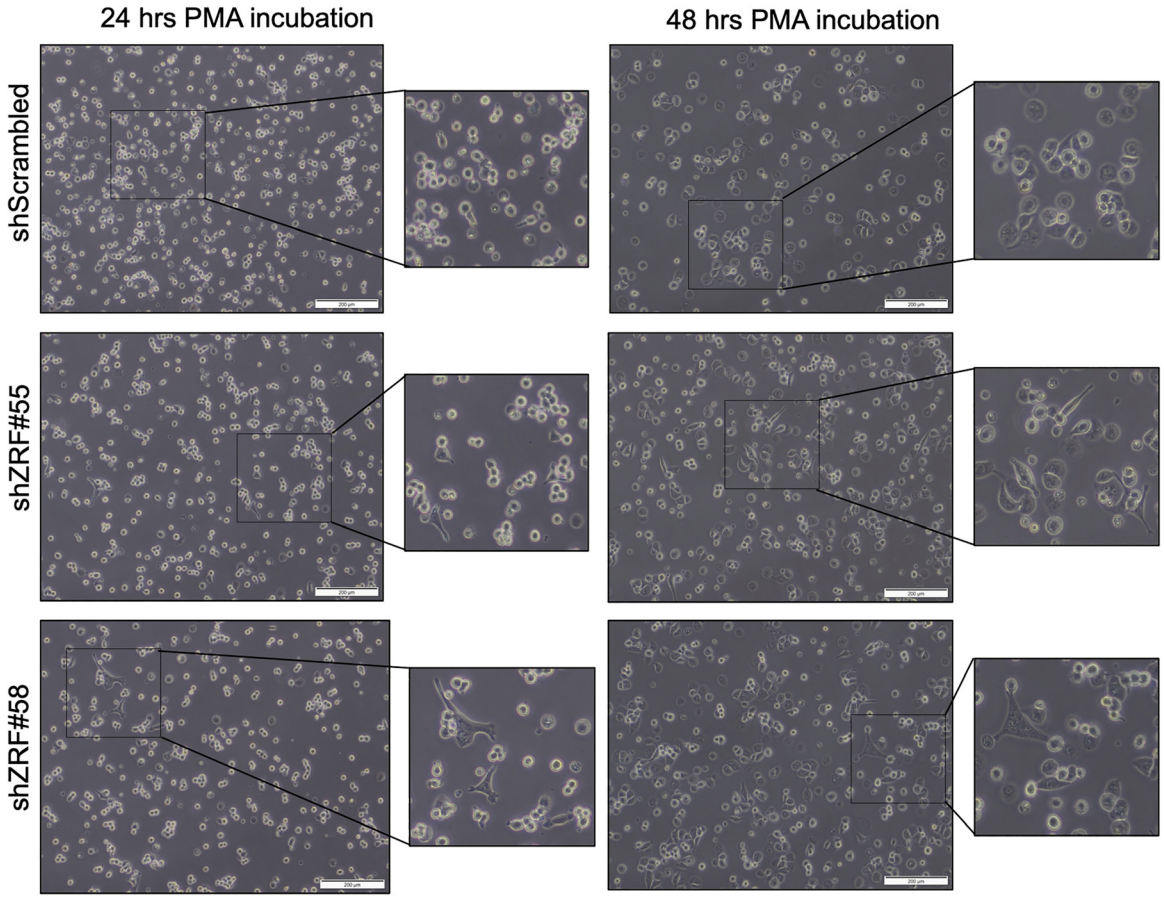

Figure 3: Morphological changes of control and ZRF1 depleted THP-1 cells for 48 h of PMA incubation. Brightfield images of THP-1 cells. Scale bars, 200 µm.

and shZRF1#58 expressing knockdown cells. The expression of CD11b was assessed in all three cell lines for both monocytes and macrophages, as shown in Figure 5B, in addition to evaluating their size and granularity. A predictable shift in CD11b expression was observed during the differentiation from monocytes to macrophages. However, while a minor variation in CD11b expression was noted between the control and ZRF1-depleted cells, this difference was not statistically significant.

Evaluation of ZRF1's effect on cell proliferation in THP-1 monocytes and PMA-differentiated macrophages

ZRF1 has been shown to control cell proliferation via the cell cycle in cancer and senescence context in different papers. To evaluate whether ZRF1 exerts a similar effect on THP-1 cells, cell proliferation experiments were conducted using both THP-1 monocytes and PMA-differentiated macrophages. THP-1 monocytes were seeded, and an MTS assay was applied to assess cell numbers on days 1, 3, 5, and 7 (Figure 6A and C). At most time points, cell numbers of ZRF1 depleted monocyte cells were significantly higher compared to control cells. This effect became more pronounced over the days. For THP-1 macrophages, experiments were carried out to evaluate ZRF1's effect after a 48 h PMA treatment and a subsequent 48 h rest period following PMA removal. The cell numbers of ZRF1 depleted macrophage cells were found to be significantly higher compared to control cells at each time point (Figure 6B and D). Macrophages derived from three cell lines continued to proliferate during the 48 h of PMA treatment. However, no increase in cell numbers was observed after PMA removal, suggesting that the cells, while metabolically active, were likely in a senescence state.

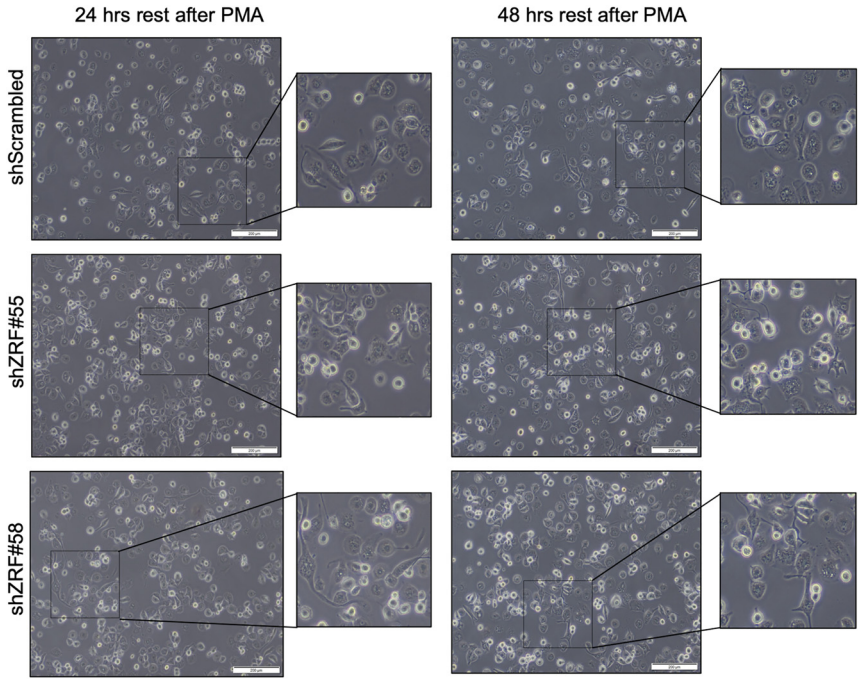

Figure 4: Morphological changes of control and ZRF1 depleted THP-1 cells for 48 h of rest period after PMA removal. Brightfield images of THP-1 cells. Scale bars, 200 µm.

Evaluation of ZRF1's effect on cell cycle in THP-1 monocytes and PMA-differentiated macrophages

Considering the ZRF1's role in modulating the cell cycle, particularly through its control of the *p16*, *INK4-ARF* locus [14, 16], and its influence on cellular senescence [16, 17], cell cycle experiments were performed on both THP-1 monocytes and macrophages derived from control and ZRF1 depleted cells (Figure 7). Flow cytometry analysis of THP-1 monocytes revealed that all three cell lines had comparable profiles, except for THP-1 cells expressing shZRF1#55. These cells showed an average of 46 % of cells in the S phase, in contrast to an average of 41 % in control cells. The influence of ZRF1 on the cell cycle was more evident when THP-1 cells differentiated into macrophages. Initially, a significant G2/M phase block was observed in all macrophages following PMA treatment, as previously reported in the literature [35]. Among all three cell lines, THP-1 cells expressing shZRF1#58 showed a distinctly different profile compared to control and other ZRF1 knockdown cells. While control cells had an average of 39 % of cells in the G2-M phase, THP-1 cells expressing shZRF1#58 had an average of 32 % in the same phase following a 48 h PMA incubation. Conversely, THP-1 cells expressing shZRF1#58 exhibited an average of 59 % of cells in the G0-G1 phase, compared to an average of 45 % in control cells after the same incubation period. Additionally, these cells had an average of 9 % of cells in the S phase, whereas control cells had an average of 15 %. Interestingly, THP-1 cells expressing shZRF1#55 displayed a cell cycle profile somewhat similar to that of control cells, positioning between wild-type and THP-1 cells expressing shZRF1#58. After a 48-h rest period post-PMA removal, control cells showed an average of 51 % of cells in the G0-G1 phase, in contrast to 66 % for THP-1 cells expressing shZRF1#58. However, the percentage of cells in the S phase remained unchanged post-PMA removal. These findings collectively indicate that ZRF1 has a more marked effect on the G0-G1 phase compared to the G2-M phase during the PMA-induced differentiation of monocytes into macrophages. Moreover, in the absence of any stimulatory effect, ZRF1 depletion appears to influence the S phase, potentially conferring advantages to actively dividing monocytes.

Discussion

ZRF1 is a multifaceted protein, is essential for chromatin remodeling and regulating gene expression. Its increasing recognition in critical cellular processes such as differentiation, proliferation, and cell cycle control has elevated its status in the realms of biological and medical research. The focus of our research was to unveil the unexplored roles of ZRF1 in the differentiation of immune cells, particularly those originating from myeloid lineage, owing to its involvement in the development of mesoderm-derived tissues and its links to hematological malignancies. Emphasizing this, our study concentrated on examining ZRF1's influence on monocyte-to-

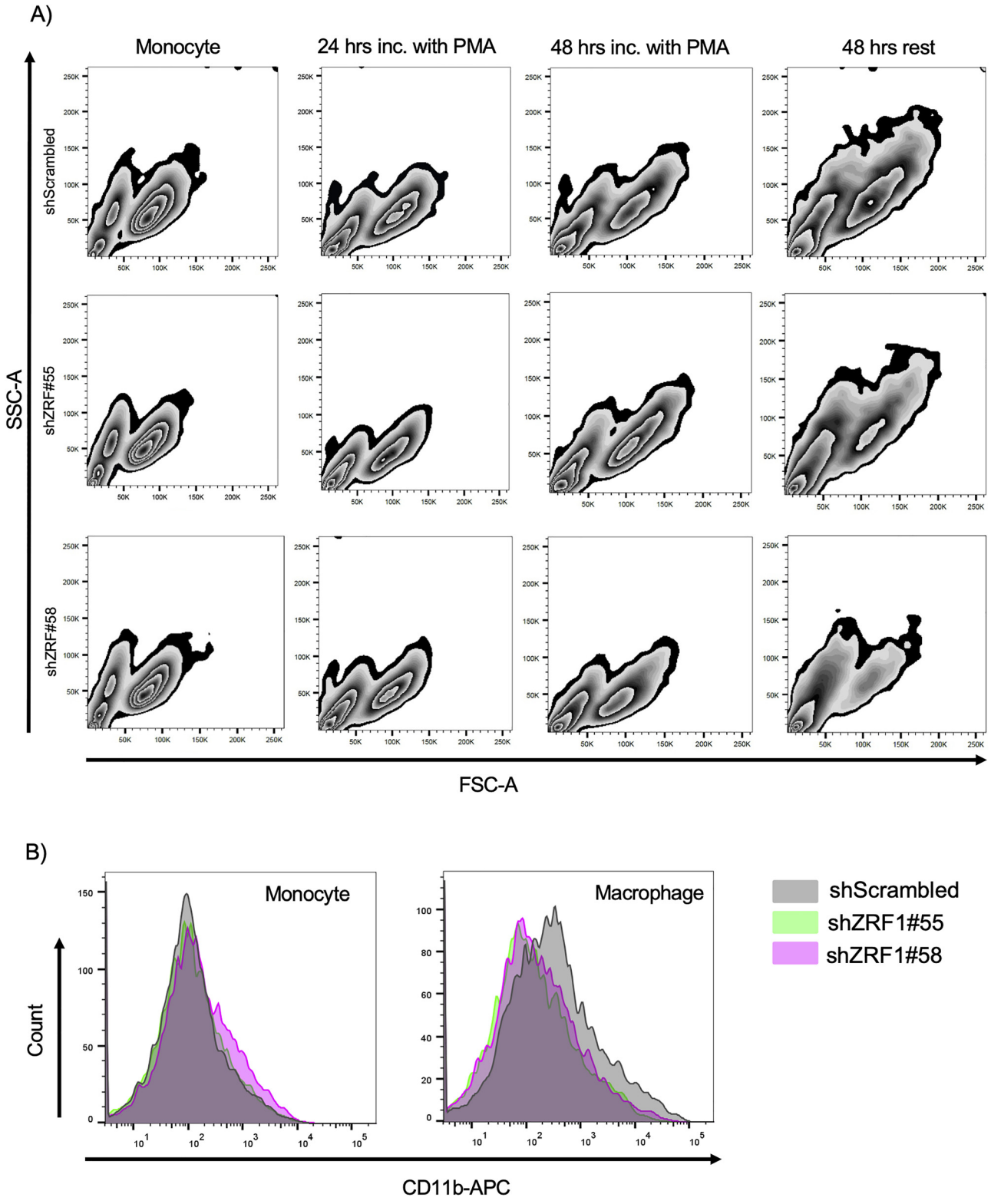

Figure 5: Flow cytometry analysis of THP-1 monocytes and macrophages derived from control and ZRF1 depleted cells. (A) Flow cytometric cell features of both monocytes and PMA-differentiated THP-1 cells expressing control and shZRF1 plasmids are shown by zebra plots displaying side scatter area (SSC-A) on the y-axis against forward scatter area (FSC-A) on the x-axis. (B) Representative images of cells stained with cell surface marker CD11b-APC for monocytes and macrophages corresponding to 48 h of rest periods after PMA removal.

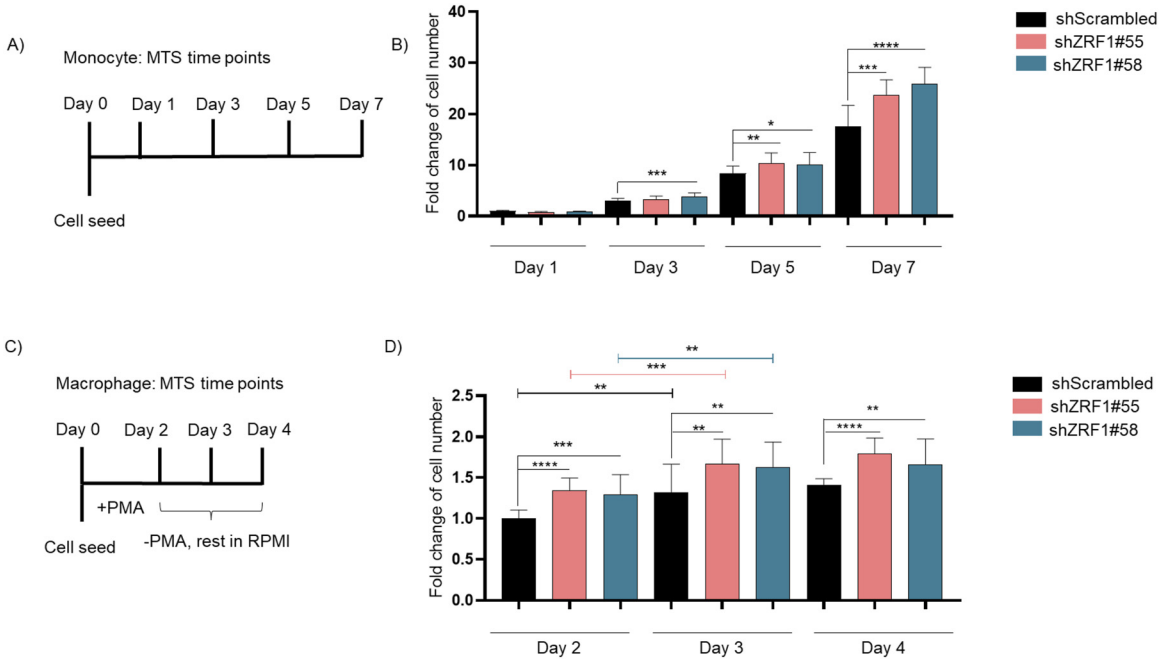

Figure 6: Cell proliferation analysis of THP-1 monocytes and macrophages in ZRF1 knockdown background. (A) Experimental plan for MTS experiments in THP-1 monocytes. (B) Experimental plan for MTS experiments in THP-1 macrophages. (C) Cell proliferation analysis for control and ZRF1 depleted THP-1 monocytes for 7 days. Cell numbers are represented as fold change and the average of three experiments, S.E.M. *p<0.05, **p<0.01, ***p<0.001, and ****p<0.0001, calculated by two-tailed unpaired t test. (D) Cell proliferation analysis for control and ZRF1 depleted THP-1 macrophages for 4 days. Cell numbers are represented as fold change and the average of three experiments, S.E.M. **p<0.01, ***p<0.001, and ****p<0.0001, calculated by two-tailed unpaired t test.

macrophage differentiation, as well as its specific roles in cell proliferation and cell cycle dynamics, utilizing THP-1 cells as a model.

Our findings revealed that the absence of ZRF1 leads to morphological alterations in THP-1 cells during their differentiation into macrophages. The control cells maintained a typical small and round shape, whereas the cells lacking ZRF1 developed a distinct spiky morphology. Notably, these ZRF1-deficient cells were characterized by a reduced size and granularity, indicating a disruption in the normal differentiation pathway. This observation is in line with the known functions of ZRF1 in cellular differentiation and development.

In the aspect of cell proliferation, a notable increase in the proliferation rate of cells was observed following the knockdown of ZRF1, compared to control groups. This trend became more evident as time progressed, highlighting ZRF1's influence on the proliferation of THP-1 monocytes and macrophages. The absence of ZRF1 appears to allow cells to bypass certain regulatory checkpoints, leading to enhanced proliferation. These findings align with previous research underscoring ZRF1's involvement in cellular senescence in the mammalian target of rapamycin (mTOR) pathway, as well as in oncogene or UV-induced senescence scenarios. As earlier studies indicated, ZRF1 depletion results in the evasion of senescence and fosters cell proliferation, primarily through the regulation of the *INK4-ARF* locus, particularly *p16*. However, for some cancer types, the absence of ZRF1 is typically linked with reduced cell proliferation. Concerning cell cycle analysis, an expected G2/M phase arrest was noted in all macrophages treated with PMA. Yet, ZRF1-deficient cells exhibited a distinct pattern, especially in the G0-G1 phase, signifying ZRF1's effect on this phase during monocyte-to-macrophage differentiation. Interestingly, during this differentiation process, ZRF1 absence didn't confer an advantage in transitioning from G1 to S phase, contrary to previous assumptions of decreased checkpoint inhibitor proteins. Instead, cells lacking ZRF1 accumulated in the G0-G1 phase, extending the understood roles of ZRF1 beyond just oncogene-induced senescence and tumor suppression. Overall, these results suggest that ZRF1 plays a rather complex, context-dependent role in cell cycle regulation and cell proliferation. They underscore the need for specifically designed experiments, considering different cell lines and treatments, to deepen the understanding of ZRF1's functions in these processes.

In summary, our research provides significant insights into ZRF1's role in the differentiation of monocytes into

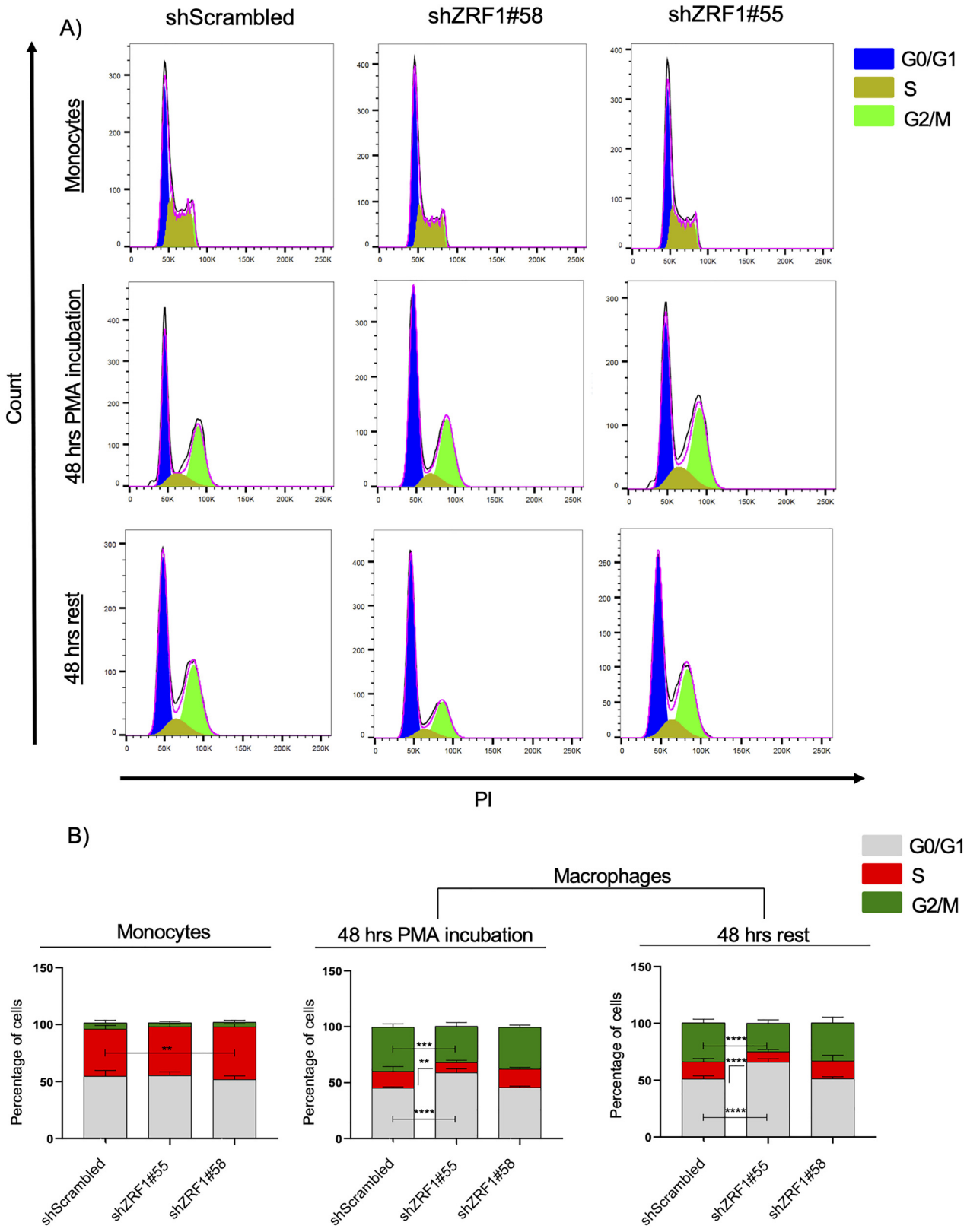

Figure 7: Cell cycle analysis of THP-1 monocytes and macrophages in ZRF1 knockdown background. (A) Representative images of cell cycle assays of THP-1 monocytes and macrophages corresponding to 48 h of PMA incubation and 48 h of rest periods after PMA removal. (B) Graphical representation of cell cycle distribution of control and ZRF1 depleted cells as both monocytes and macrophages. Data represent the average of three experiments, ± S.E.M. **p<0.01, ***p<0.001, and ****p<0.0001 calculated by two-tailed unpaired *t* test.

macrophages, and its influence on cell proliferation and the cell cycle. These findings not only corroborate with the existing knowledge about ZRF1 but also expand our understanding of its diverse roles in cellular processes. The complexities of ZRF1's functions in various cellular contexts and its potential as a therapeutic target necessitate further research.

Acknowledgments: We are grateful to the IBG Flow Cytometry and Cell Sorting Unit for their expert help and assistance. We would like to thank Dr. Luciano Di Croce for plasmids, Prof. Dr. Güneş Esendağlı for THP-1 cells and Prof. Dr. Şerif Şentürk for shRNA plasmid and HEK293T cells. We thank the members of the Department of Biochemistry at Faculty of Pharmacy at Ege University for their support.

Research ethics: No ethical approval was needed since it is a cell culture study.

Informed consent: No informed consent and ethical committee form are needed since it is a cell culture study.

Author contributions: The authors have accepted responsibility for the entire content of this manuscript and approved its submission. AKO conceived and designed the experiments. AKO and MB performed all experiments and analyzed the data. AKO wrote the paper.

Competing interests: Authors state no conflict of interest.

Research funding: This study was funded by the Scientific and Technological Research Council of Turkey (TUBITAK) 1002 Grant No. 222Z173.

Data availability: The raw data can be obtained on request from the corresponding author.

References

1. Papadopoulou T, Kaymak A, Sayols S, Richly H. Dual role of Med12 in PRC1-dependent gene repression and ncRNA-mediated transcriptional activation. Cell Cycle 2016;15:1479–93.
2. Richly H, Rocha-Viegas L, Ribeiro JD, Demajo S, Gundem G, Lopez-Bigas N, et al. Transcriptional activation of polycomb-repressed genes by ZRF1. Nature 2010;468:1124–8.
3. Chitale S, Richly H. DICER and ZRF1 contribute to chromatin decondensation during nucleotide excision repair. Nucleic Acids Res 2017;45:5901–12.
4. Gracheva E, Chitale S, Wilhelm T, Rapp A, Byrne J, Stadler J, et al. ZRF1 mediates remodeling of E3 ligases at DNA lesion sites during nucleotide excision repair. J Cell Biol 2016;213:185–200.
5. Richly H, Di Croce L. The flip side of the coin: role of ZRF1 and histone H2A ubiquitination in transcriptional activation. Cell Cycle 2011;10: 745–50.
6. Qiu XB, Shao YM, Miao S, Wang L. The diversity of the DnaJ/Hsp40 family, the crucial partners for Hsp70 chaperones. Cell Mol Life Sci 2006;63:2560–70.
7. Jaiswal H, Conz C, Otto H, Wölfle T, Fitzke E, Mayer MP, et al. The chaperone network connected to human ribosome-associated complex. Mol Cell Biol 2011;31:1160–73.
8. Chen DH, Huang Y, Liu C, Ruan Y, Shen WH. Functional conservation and divergence of J-domain-containing ZUO1/ZRF orthologs throughout evolution. Planta 2014;239:1159–73.
9. Aloia L, Di Stefano B, Sessa A, Morey L, Santanach A, Gutierrez A, et al. Zrf1 is required to establish and maintain neural progenitor identity. Genes Dev 2014;28:182–97.
10. Aloia L, Gutierrez A, Caballero JM, Di Croce L. Direct interaction between Id1 and Zrf1 controls neural differentiation of embryonic stem cells. EMBO Rep 2015;16:63–70.
11. Feng J, Chen D, Berr A, Shen WH. ZRF1 chromatin regulators have polycomb silencing and independent roles in development. Plant Physiol 2016;172:1746–59.
12. Kaymak A, Richly H. Zrf1 controls mesoderm lineage genes and cardiomyocyte differentiation. Cell Cycle 2016;15:3306–17.
13. Helary L, Castille J, Passet B, Vaiman A, Beauvallet C, Jaffrezic F, et al. DNAJC2 is required for mouse early embryonic development. Biochem Biophys Res Commun 2019;516:258–63.
14. Barilari M, Bonfils G, Treins C, Koka V, De Villeneuve D, Fabrega S, et al. ZRF1 is a novel S6 kinase substrate that drives the senescence programme. EMBO J 2017;36:736–50.
15. Serrano M, Hannon GJ, Beach D. A new regulatory motif in cell-cycle control causing specific inhibition of cyclin D/CDK4. Nature 1993;366: 704–7.
16. Ribeiro JD, Morey L, Mas A, Gutierrez A, Luis NM, Mejetta S, et al. ZRF1 controls oncogene-induced senescence through the INK4-ARF locus. Oncogene 2013;32:2161–8.
17. De Magis A, Limmer M, Mudiyam V, Monchaud D, Juranek S, Paeschke K. UV-induced G4 DNA structures recruit ZRF1 which prevents UV-induced senescence. Nat Commun 2023;14:6705.
18. Dyachenko L, Havrysh K, Lytovchenko A, Dosenko I, Antoniuk S, Filonenko V, et al. Autoantibody response to ZRF1 and KRR1 SEREX antigens in patients with breast tumors of different histological types and grades. Dis Markers 2016;2016:5128720.
19. Kaymak A, Sayols S, Papadopoulou T, Richly H. Role for the transcriptional activator ZRF1 in early metastatic events in breast cancer progression and endocrine resistance. Oncotarget 2018;9:28666–90.
20. Liu H, Li J, Zhao H, Liu X, Ye X. DNAJC2 is reversely regulated by miR-627-3p, promoting the proliferation of colorectal cancer. Mol Med Rep 2021; 24:589.
21. Imamura T, Komatsu S, Ichikawa D, Miyamae M, Okajima W, Ohashi T, et al. Overexpression of ZRF1 is related to tumor malignant potential and a poor outcome of gastric carcinoma. Carcinogenesis 2018;39: 263–71.
22. Demajo S, Uribesalgo I, Gutiérrez A, Ballaré C, Capdevila S, Roth M, et al. ZRF1 controls the retinoic acid pathway and regulates leukemogenic potential in acute myeloid leukemia. Oncogene 2014; 33:5501–10.
23. Greiner J, Ringhoffer M, Taniguchi M, Hauser T, Schmitt A, Döhner H, et al. Characterization of several leukemia-associated antigens inducing humoral immune responses in acute and chronic myeloid leukemia. Int J Cancer 2003;106:224–31.
24. Al Qudaihi G, Lehe C, Dickinson A, Eltayeb K, Rasheed W, Chaudhri N, et al. Identification of a novel peptide derived from the M-phase phosphoprotein 11 (MPP11) leukemic antigen recognized by human CD8+ cytotoxic T lymphocytes. Hematol Oncol Stem Cell Ther 2010;3: 24–33.
25. Yi L, Li Z, Hu T, Liu J, Li N, Cao X, et al. Intracellular HSP70L1 inhibits human dendritic cell maturation by promoting suppressive H3K27me3 and H2AK119Ub1 histone modifications. Cell Mol Immunol 2020;17: 85–94.

26. Auwerx J. The human leukemia cell line, THP-1: a multifacetted model for the study of monocyte-macrophage differentiation. Experientia 1991;47:22–31.
27. Bosshart H, Heinzelmann M. THP-1 cells as a model for human monocytes. Ann Transl Med 2016;4:438.
28. Qin Z. The use of THP-1 cells as a model for mimicking the function and regulation of monocytes and macrophages in the vasculature. Atherosclerosis 2012;221:2–11.
29. Tedesco S, De Majo F, Kim J, Trenti A, Trevisi L, Fadini GP, et al. Convenience versus biological significance: are PMA-differentiated THP-1 cells a reliable substitute for blood-derived macrophages when studying in vitro polarization? Front Pharmacol 2018;9:71.
30. Baxter EW, Graham AE, Re NA, Carr IM, Robinson JI, Mackie SL, et al. Standardized protocols for differentiation of THP-1 cells to macrophages with distinct M(IFNγ+LPS), M(IL-4) and M(IL-10) phenotypes. J Immunol Methods 2020;478:112721.
31. Lund ME, To J, O'Brien BA, Donnelly S. The choice of phorbol 12-myristate 13-acetate differentiation protocol influences the response of THP-1 macrophages to a pro-inflammatory stimulus. J Immunol Methods 2016;430:64–70.
32. Park EK, Jung HS, Yang HI, Yoo MC, Kim C, Kim KS. Optimized THP-1 differentiation is required for the detection of responses to weak stimuli. Inflamm Res 2007;56:45–50.
33. Genin M, Clement F, Fattaccioli A, Raes M, Michiels C. M1 and M2 macrophages derived from THP-1 cells differentially modulate the response of cancer cells to etoposide. BMC Cancer 2015;15:577.
34. Forrester MA, Wassall HJ, Hall LS, Cao H, Wilson HM, Barker RN, et al. Similarities and differences in surface receptor expression by THP-1 monocytes and differentiated macrophages polarized using seven different conditioning regimens. Cell Immunol 2018;332: 58–76.
35. Gažová I, Lefevre L, Bush SJ, Clohisey S, Arner E, de Hoon M, et al. The transcriptional network that controls growth arrest and macrophage differentiation in the human myeloid leukemia cell line thp-1. Front Cell Dev Biol 2020;8:498.